frontiers | Frontiers in Earth Science

TYPE Original Research
PUBLISHED 04 August 2022
DOI 10.3389/feart.2022.914432

OPEN ACCESS

EDITED BY
Haijun Song,
China University of Geosciences
Wuhan, China

REVIEWED BY
Mao Luo,
Nanjing Institute of Geology and
Paleontology (CAS), China
Feifei Zhang,
Nanjing University, China

*CORRESPONDENCE
Xiaolin Zhang,
zhxl2012@ustc.edu.cn
Menghan Li,
limh@ustc.edu.cn

SPECIALTY SECTION
This article was submitted to
Geochemistry,
a section of the journal
Frontiers in Earth Science

RECEIVED 06 April 2022
ACCEPTED 11 July 2022
PUBLISHED 04 August 2022

CITATION
Huang X, Li D, Zhang X, Xu Y, Sun L, Li M and Shen Y (2022), High resolution C-isotopic data from microbialites in the aftermath of the end-Permian mass extinction in South China.
Front. Earth Sci. 10:914432.
doi: 10.3389/feart.2022.914432

High resolution C-isotopic data from microbialites in the aftermath of the end-Permian mass extinction in South China

Xiemin Huang, Dandan Li, Xiaolin Zhang*, Yilun Xu, Lilin Sun, Menghan Li* and Yanan Shen

School of Earth and Space Sciences, University of Science and Technology of China, Hefei, China

Globally, Late Permian to Early Triassic carbonate rocks record several pronounced positive and negative C-isotope excursions, indicating a dramatic reorganization of the global carbon cycle. These C-isotopic anomalies provide important constraints on environmental changes that occurred during the end-Permian extinction and the subsequent delayed biotic recovery. In this study, we present high-resolution carbonate C-isotopic data ($\delta^{13}C_{carb}$) spanning the Permian-Triassic transition at Dajiang, South China. Our results reveal a general decrease in $\delta^{13}C_{carb}$ of ~3.3‰ during the microbialite formation which was followed by an increase. C-isotopic chemostratigraphic correlation between the Dajiang section and the Global Boundary Stratotype Section and Point (GSSP) at Meishan suggest a hiatus of several thousands of years between the pre-extinction skeletal limestones and the microbialite deposition in the aftermath of the end-Permian extinction in South China. We suggest that multiple sources of ^{13}C-depleted dissolved carbon are required to explain the negative $\delta^{13}C_{carb}$ excursions as well as the $\delta^{13}C_{carb}$ differences among microbialites deposited in various paleogeographic locations. Our study shows that carbon cycles during the formation of microbialite may have been more complex than previously thought, and cessation of microbialite formation may have been controlled by both global and local environmental changes.

KEYWORDS

Carbon isotopes, End-Permian mass extinction, Microbialite, ^{13}C-depleted carbon, South China

Introduction

The end-Permian mass extinction (~252 Ma), was the most severe biotic crisis of the Phanerozoic, which eliminated over 90% of marine species and fundamentally altered marine ecosystems (Knoll et al., 2007; Song et al., 2012, 2018). It is generally accepted that environmental deterioration, triggered by the eruption of the Siberian Traps Large Igneous Province, may have led to the end-Permian mass extinction (Kamo et al., 2003; Svensen et al., 2009; Grasby et al., 2011; Shen et al., 2011; Burgess et al., 2017; Zhang

et al., 2017; Fielding et al., 2019; Li et al., 2021, 2022). C-isotopic changes in space and time have been instrumental in understanding the environmental changes that occurred during Late Permian–Early Triassic transition (e.g., Grasby and Beauchamp, 2008; Meyer et al., 2011; Grasby et al., 2013; Song et al., 2013). Existing data show large perturbations of global carbon cycles during the end-Permian mass extinction and the delayed Early Triassic biotic recovery (e.g., Payne et al., 2004; Xie et al., 2007). For example, a pronounced negative C-isotopic excursion coincided with the end-Permian extinction worldwide (Holser et al., 1989; Cao et al., 2002, 2009). The sources of the ^{13}C-depleted carbon causing this global negative C-isotopic excursion are argued to have come from volcanic emissions of CO_2 (Payne and Kump, 2007; Cao et al., 2009), the oxidation of methane (Ryskin, 2003), the increase of ^{12}C-enriched organic carbon weathering due to eustatic sea-level fall (Holser et al., 1989), the incursion of ^{12}C-enriched dissolved carbon in anoxic/euxinic deep water into the shallow marine environment (Riccardi et al., 2007; Zhang et al., 2021), amongst others. However, $\delta^{13}C$ data from the Permian-Triassic transition indicate that $\delta^{13}C_{carb}$ compositions continued to decrease following the end-Permian mass extinction level, when microbialites were deposited (Krull et al., 2004; Mu et al., 2009; Wang et al., 2009; Liao et al., 2010; Liu et al., 2010; Luo et al., 2010, 2011; Yang et al., 2011; Wu et al., 2017).

Permian-Triassic microbialites are carbonates rich in microbial structures and cements of various forms including stromatolites, thrombolites and dendrolites, that were deposited in the aftermath of the end-Permian mass extinction (Lehrmann 1999; Wang et al., 2005; Baud et al., 2007; Kershaw et al., 2007, 2012; Yang et al., 2011; Wang et al., 2019). Most of the Permian-Triassic microbialites were developed in the low-latitude Tethys Ocean, especially in South China where many excellent sections are exposed. Extensively multidisciplinary studies have greatly improved our knowledge about the age, microbial structure, genesis, and environmental implications of these microbialites (Wang et al., 2005; Luo et al., 2010; Wang et al., 2016; Deng et al., 2017; Pei et al., 2019). For example, all of the C-isotopic profiles from South China have shown that the $\delta^{13}C_{carb}$ compositions continue to decrease from pre-extinction bioclastic limestones enriched in benthic fossils to the overlying microbialites (e.g., Yang et al., 2011).

In this study, we report high-resolution $\delta^{13}C_{carb}$ data of microbialites from the Dajiang section in South China. The microbialite interval is about 14.5 m in the Dajiang section and might be the thickest in South China, which could reveal more details of C-isotopic variations during this period. We aim to better understand environmental significance of C-isotopic variations in microbialites and their possible link to the delayed biotic recovery from the end-Permian mass extinction.

Geological background and stratigraphy

During the Permian-Triassic transition, the South China craton, including the Yangtze and Cathaysia blocks, was situated north of the paleo-equator in the eastern part of the Paleotethys Ocean (Figure 1A). The Nanpanjiang Basin is a deep-marine embayment in the Yangtze Platform, which opened south-eastward to the Panthalassa Ocean (Lehrmann, 1999). The Great Bank of Guizhou, which evolved as an isolated carbonate platform within the Nanpanjiang Basin, preserved continuous shallow marine deposition from the late Permian to the middle Triassic (Lehrmann et al., 2003). There are many outstanding sections that preserved microbialites in the Nanpanjiang Basin (Luo et al., 2011, 2014). In part because of its thickness and excellent exposure, the Dajiang microbialites were the focus of this study.

The Dajiang section (106°39′49″E, 25°33′47″N) is located in Bianyang town, Luodian County, Guizhou Province. Paleogeographically, the study section was situated on the Great Bank of Guizhou and was deposited at a water depth possibly less than 100 m (Song et al., 2013) (Figure 1B). The Dajiang section comprises, in ascending order, the upper Permian Wujiaping Formation and the lower Triassic Daye Formation (Figure 2). The uppermost Wujiaping Formation is characterized by skeletal limestone, and contains abundant shallow-marine fossils such as fusulinids, foraminifera, brachiopods, and calcareous algae (Lehrmann et al., 2003). At the base of the Daye Formation, a 14.5 m thick microbialite was deposited, which is mainly composed of laminar or spotted thrombolites (Figure 2). The microbialite deposit is overlain by grainstone and packstone (Jiang et al., 2014).

It is widely accepted that the end-Permian extinction level is correlated with bed 25 in the GSSP at Meishan, South China and the Permian-Triassic boundary (PTB) is correlated with bed 27c at Meishan, indicated by the first appearance datum (FAD) of the conodont species *Hindeodus parvus* (Yin et al., 2001). However, the position of the FAD of *H. parvus* in the Dajiang section was placed at different levels, and therefore the exact placement of the PTB remains debated (Jiang et al., 2014; Lehrmann et al., 2015; Zhang et al., 2020). The PTB has been placed either at the uppermost of the Wujiaping Formation (Jiang et al., 2014) or within the microbialite (Lehrmann et al., 2015; Zhang et al., 2020). In this study, we follow the scheme of Jiang et al. (2014) (Figure 2). Regardless of the precise PTB level, there is little doubt that the microbialites at Dajiang were deposited in the aftermath of the end-Permian mass extinction.

Materials and methods

A total of 100 bulk samples were collected continuously over ~23.4-m of strata across the PTB in the Dajiang section. All

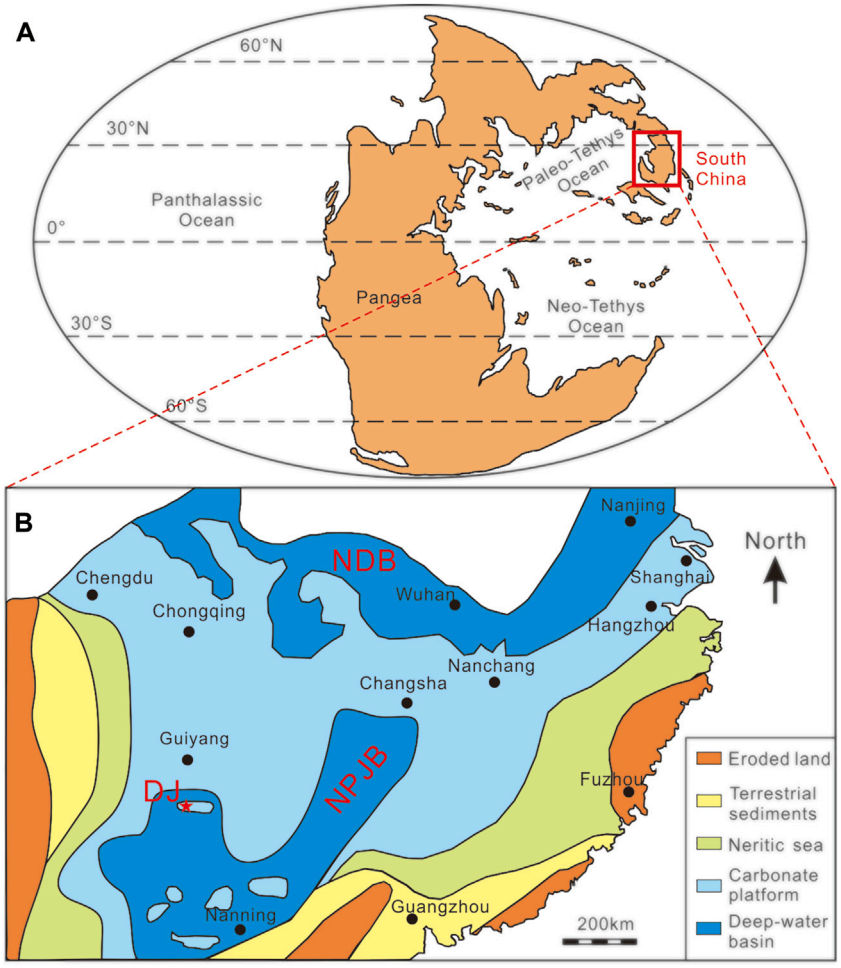

FIGURE 1
Permian-Triassic paleogeographic sketch map of the world **(A)** and the South China Craton **(B)**. Inset red rectangle in **(A)** shows the area of the South China Craton. The red star in **(B)** shows the location of the Dajiang section. Paleogeography of the world is revised from Shen et al. (2015), and the map of the South China Craton is modified from Xie et al. (2010) and Yin et al. (2014). DJ: Dajiang section; NDB: Northern Deepwater Basin; NPJB: Nanpanjiang Basin.

sample depths are measured relative to the PTB. Among them, 16 samples are from the skeletal limestone interval (−3.1–0 m), 66 samples are from the microbialite interval (0–14.5 m), and 18 samples are from the grainstone and packstone (14.5–20.3 m) (Figure 2). Prior to isotopic analysis, any weathered surfaces and visible calcite veins were trimmed off. Pieces of the crushed samples were then ground to fine powders (<200 mesh) using an automated agate mortar and pestle device. Sample preparation and analyses were performed in the Biogeochemical Laboratory at University of Science and Technology of China.

For $\delta^{13}C_{carb}$ and $\delta^{18}O_{carb}$ analysis, approximately 150 μg of sample powder was reacted with 102–105% anhydrous phosphoric acid at 70°C in a Kiel IV carbonate device to generate CO_2. The evolved CO_2 gas was purified in a cryogenic cleaning device and then measured on a ThermoFinnigan MAT 253 Mass Spectrometer. The carbon and oxygen isotope compositions are expressed in the conventional delta notation as per mil (‰) deviations relative to the V-PDB standard. Analytical reproducibility was monitored by replicate analysis of a Chinese national standard GBW04416 ($\delta^{13}C_{carb}$ = +1.61‰, $\delta^{18}O_{carb}$ = −11.59‰), and was better than ±0.05‰ for $\delta^{13}C_{carb}$ and ±0.06‰ for $\delta^{18}O_{carb}$.

Results and data evaluation

The $\delta^{13}C_{carb}$ data show large variations during the Permian–Triassic transition in the Dajiang section, ranging from −0.44‰ to +2.87‰ (Supplementary Table S1; Figure 2). Post-depositional diagenetic processes can alter the primary

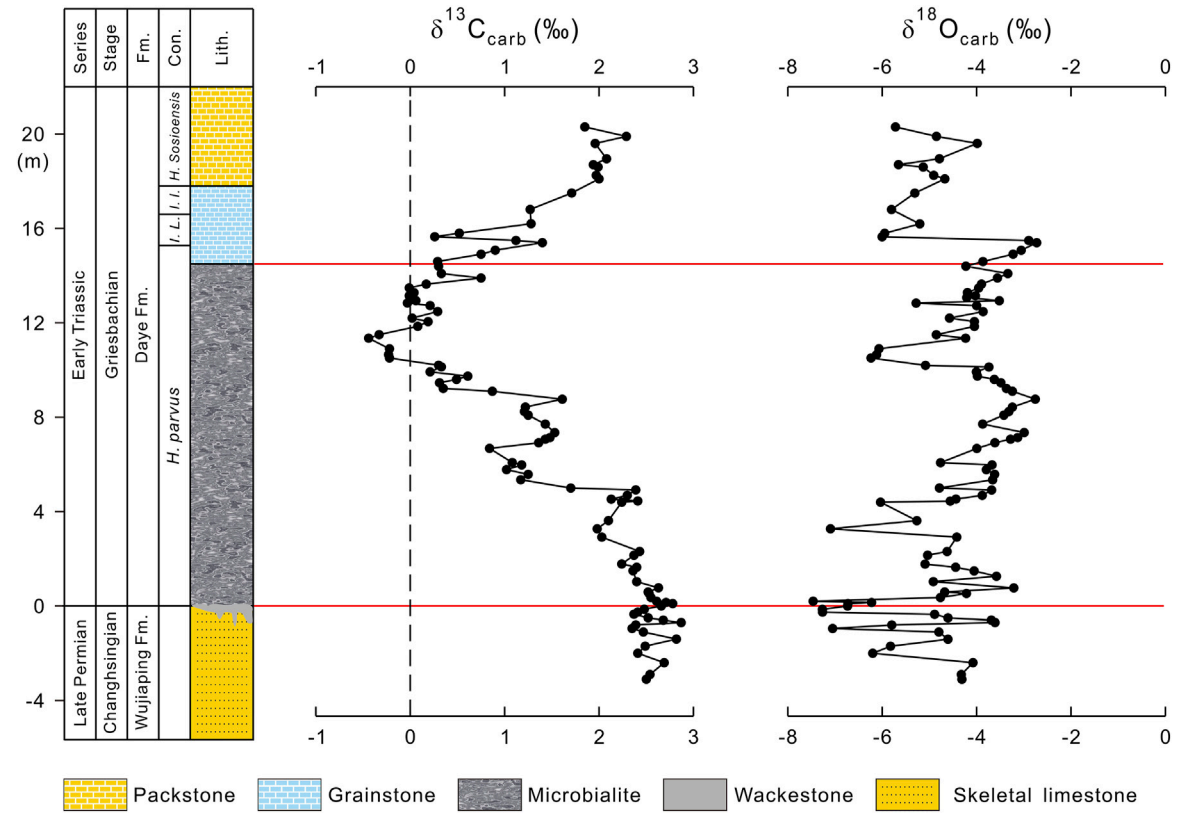

FIGURE 2
Profiles of $\delta^{13}C_{carb}$ and $\delta^{18}O_{carb}$ from the Dajiang section. Conodont zones are from Jiang et al. (2014). Abbreviations: *H. parvus* = *Hindeodus parvus* zone; *I. L.* = *Isarcicella lobate* zone; *I. I.* = *Isarcicella isarcica* zone; *H. sosioensis* = *Hindeodus sosioensis* zone; Fm. = Formation; Con. = Conodont zone; Lith. = Lithology.

C-isotopic compositions of sedimentary carbonates (Kaufman and Knoll, 1995). Therefore, diagenetic effects must be evaluated prior to the interpretation of the isotope data. It has been shown that diagenetic fluids enriched in organic-derived carbon can simultaneously alter the carbonate $\delta^{13}C$ and $\delta^{18}O$ towards more negative values, and as such, the positive correlation between $\delta^{13}C_{carb}$ and $\delta^{18}O_{carb}$ may be indicative of significant diagenetic alteration (Kaufman and Knoll, 1995). Extreme negative $\delta^{18}O_{carb}$ values (<−10‰) have also been suggested to be an additional indicator of diagenetic alteration (Kaufman and Knoll, 1995). However, the $\delta^{18}O_{carb}$ compositions from the Dajiang section range from −2.7‰ to −7.5‰, implying the primary nature for $\delta^{13}C_{carb}$.

The plot of $\delta^{13}C_{carb}$ and $\delta^{18}O_{carb}$ show moderate correlation (R^2 = 0.4653) for the pre-extinction skeletal limestone (Figure 3A). This could suggest diagenetic alteration of the primary isotopic compositions. However, the narrow $\delta^{13}C_{carb}$ range from +2.35‰ to +2.87‰ suggest that the $\delta^{13}C_{carb}$ compositions were not significantly changed and they are of primary isotopic significance, although the $\delta^{18}O_{carb}$ compositions could be altered. There is little correlation between $\delta^{13}C_{carb}$ and $\delta^{18}O_{carb}$ for the microbialites and overlying grainstones and packstones, suggesting that the primary $\delta^{13}C_{carb}$ compositions were well preserved (Figures 3B,C). Similarly, the plot between $\delta^{13}C_{carb}$ and $\delta^{18}O_{carb}$ for all samples from Dajiang shows little correlation, reinforcing the primary nature for $\delta^{13}C_{carb}$ (Figure 3D).

It is worthy to note that a preliminary $\delta^{13}C_{carb}$ study on the Dajiang section was carried out by Krull et al. (2004) (Figure 4). In general, the two datasets are consistent. However, our high-resolution sampling and precise measurements reveal more details about C-isotopic changes. As shown in Figure 2, the $\delta^{13}C_{carb}$ values of the pre-extinction skeletal limestone range from +2.35‰ to +2.87‰, with an average of +2.55‰. There is not much change in $\delta^{13}C_{carb}$ in the pre-extinction interval, although there is a slight $\delta^{13}C_{carb}$ increase from +2.41‰ to +2.78‰ (Figure 4).

After the end-Permian extinction event, the $\delta^{13}C_{carb}$ data display a broad decrease through the microbialite interval, with $\delta^{13}C_{carb}$ decreasing from +2.78‰ to −0.44‰ (Figure 2). Following this the $\delta^{13}C_{carb}$ data recover from the nadir

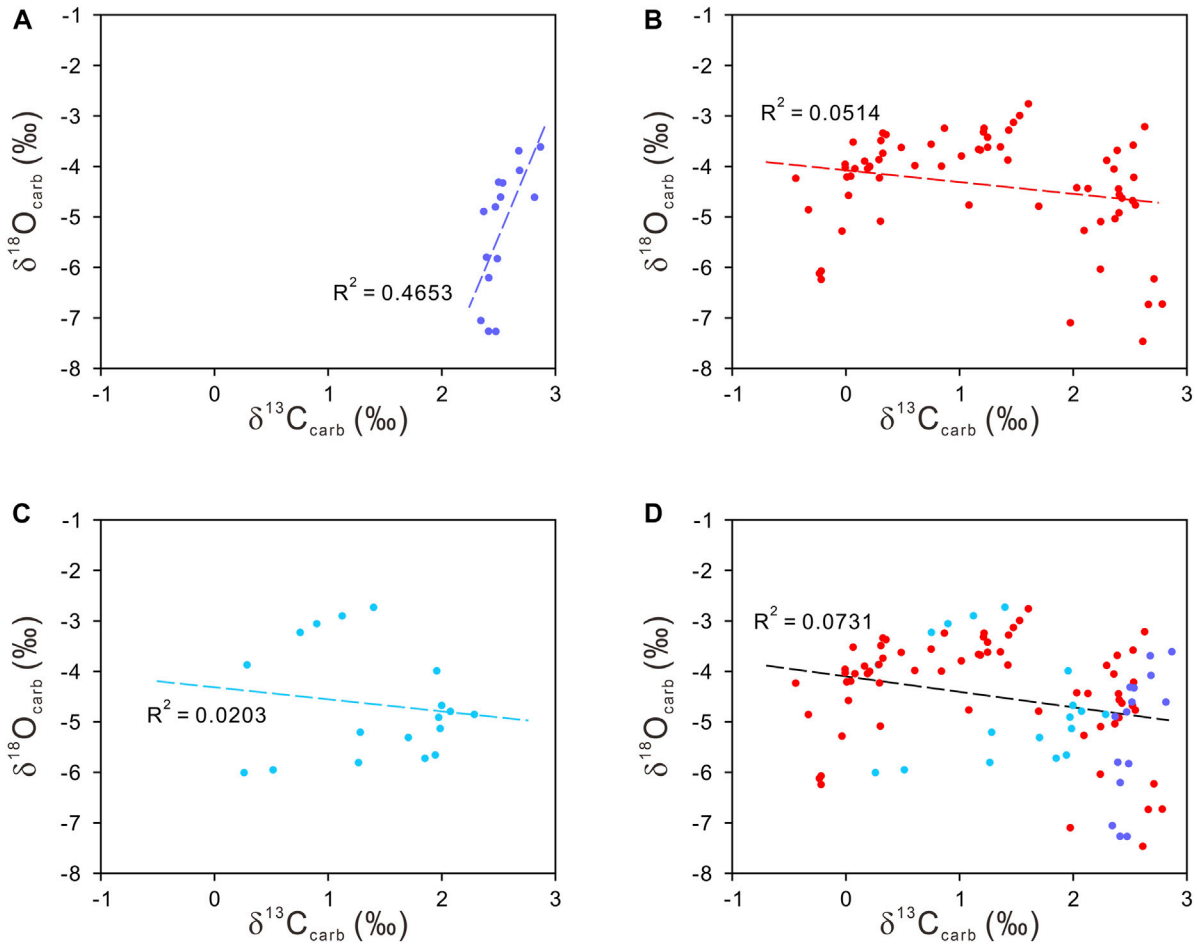

FIGURE 3
Cross-plot of $\delta^{13}C_{carb}$ and $\delta^{18}O_{carb}$ for pre-extinction skeletal limestone **(A)**, microbialites **(B)**, overlying grainstones and packstones **(C)**, and all samples from the Dajiang section **(D)**.

of −0.44‰ to +0.29‰ in the uppermost part of the microbialite interval, and continue to rise to +2.29‰ in the overlying grainstones and packstones (Figure 2).

Our high-resolution C-isotope data reveal that the broad $\delta^{13}C_{carb}$ decrease in the microbialite interval consists of three consecutive episodes (Figure 2). During episode I, $\delta^{13}C_{carb}$ slightly decreases from +2.78‰ to +1.98‰ followed by a recovery to +2.39‰ at 4.92 m (Figure 2). The $\delta^{13}C_{carb}$ continues to decrease from +2.39‰ to +0.84‰ at the height of 6.68 m during episode II, followed by an increase to +1.61‰ at 8.76 m (Figure 2). Episode III shows a $\delta^{13}C_{carb}$ decrease from +1.61‰ to the minimal value of −0.44‰ at 11.35 m in the microbialite interval (Figure 2). The $\delta^{13}C_{carb}$ increases from −0.44‰ to +0.30‰ at the uppermost of the microbialite interval and continues to increase to +2.29‰ in the overlying grainstones and packstones though a sharp negative shift from +1.40‰ at 15.4 m to +0.26‰ at 15.65 m is shown (Figure 2).

Discussion

$\delta^{13}C$ stratigraphic correlation between Dajiang and GSSP Meishan section

Microbialites were deposited immediately following the end-Permian extinction in a shallow marine carbonate environment. Like Dajiang, observations from many sections in South China indicate an erosional surface between the underlying skeletal packstone and overlying microbialite (Jiang et al., 2014) (Figure 2). This has been interpreted as submarine chemical dissolution due to ocean acidification (Payne et al., 2007; Lehrmann et al., 2015) or subaerial erosion due to the major global regression near the extinction event (e.g., Wignall et al., 2009). However, both models could work depending on the paleotopography and accommodation space of the studied section (Yin et al., 2014). It was estimated that a hiatus between the skeletal limestone and the basal microbialite may

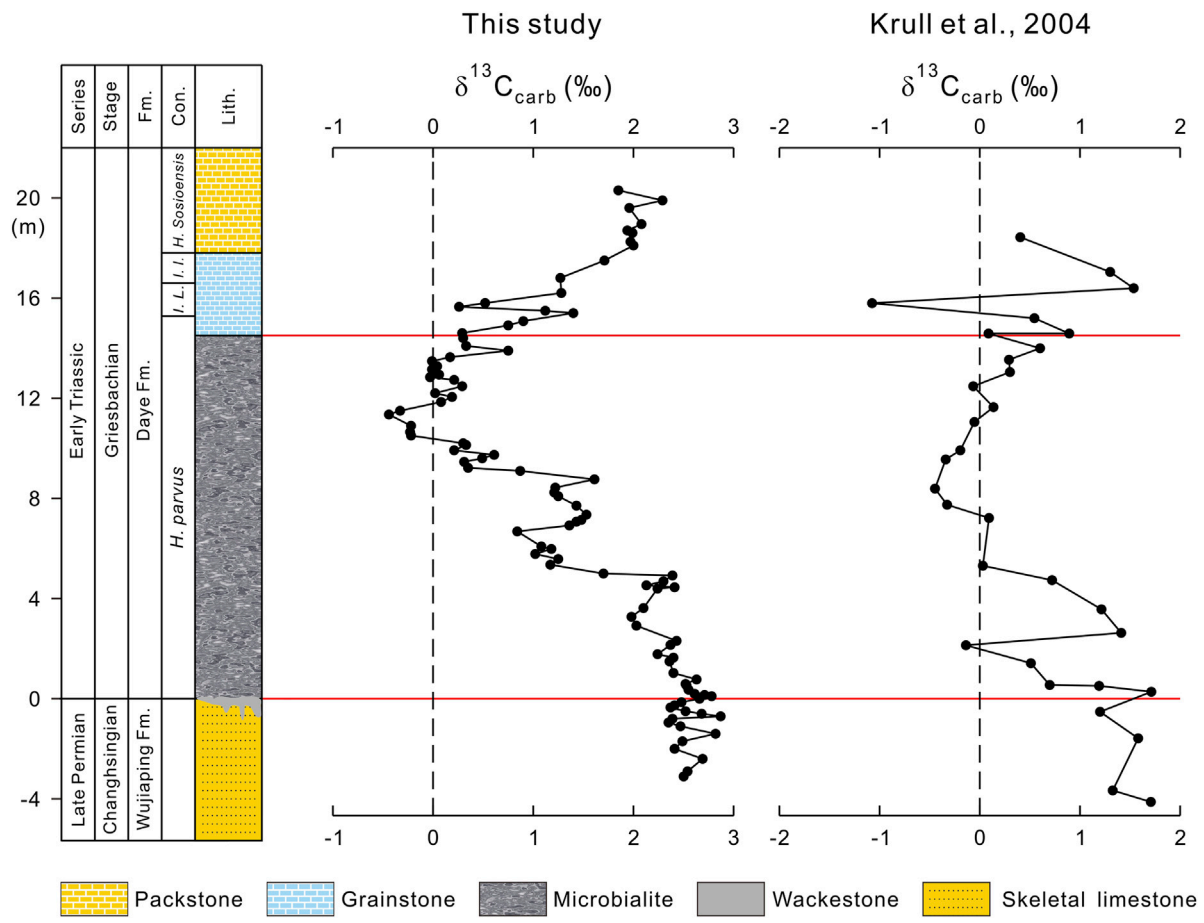

FIGURE 4
Comparison of $\delta^{13}C_{carb}$ records of the Dajiang section from this study and Krull et al. (2004).

be 50–100 ky (Yin et al., 2014). The $\delta^{13}C$ stratigraphic correlation between Dajiang and GSSP Meishan section suggest that the deposition from the skeletal packstone to the overlying microbialite at Dajiang may be not continuous (Figures 2, 5).

At Dajiang, there is minor $\delta^{13}C_{carb}$ increase from +2.37‰ to +2.78‰ from the top of the packstone to the basal microbialite (Figure 5). In contrast, a gradual $\delta^{13}C_{carb}$ decrease from the bed 23 to bed 24e, followed by another $\delta^{13}C_{carb}$ decrease of about 4‰, occurs at the extinction level at bed 25 at Meishan (Cao et al., 2002) (Figure 5). After the extinction, the $\delta^{13}C_{carb}$ at Meishan increases about 3‰, gradually from bed 25 to beds 28–29 (Cao et al., 2002) (Figure 5). However, the $\delta^{13}C_{carb}$ continues to decrease from the packstone to microbialite at Dajiang (Figures 2, 5). The Meishan section may be a condensed section which may have not recorded all of the C-isotopic changes during Permian-Triassic transition. However, the $\delta^{13}C_{carb}$ from Dajiang missed several significant $\delta^{13}C_{carb}$ changes in Meishan and elsewhere. Therefore, our $\delta^{13}C_{carb}$ data from Dajiang support that the microbialites were deposited in the aftermath of the end-Permian extinction and that the deposition of several thousands of years was probably missing prior to the microbialite formation.

$\delta^{13}C$ stratigraphic correlations of microbialites between Dajiang and elsewhere in South China

The correlations between the Dajiang section and Zuodeng and Taiping sections in the same Nanpanjiang Basin show similarities as well as differences in $\delta^{13}C$ variations (Figure 6). The $\delta^{13}C_{carb}$ from all three sections show decreasing values in the microbialite interval and increasing values after the deposition of microbialites (Figure 6). The minimal $\delta^{13}C_{carb}$ values at Dajiang, Zuodeng, and Taiping are −0.44‰, +0.3‰, and −0.7‰, respectively (Figure 6). Unlike Dajiang, the $\delta^{13}C_{carb}$ profiles of the microbialites from Zuodeng and Taiping remain relatively stable after the $\delta^{13}C_{carb}$ decrease from the pre-

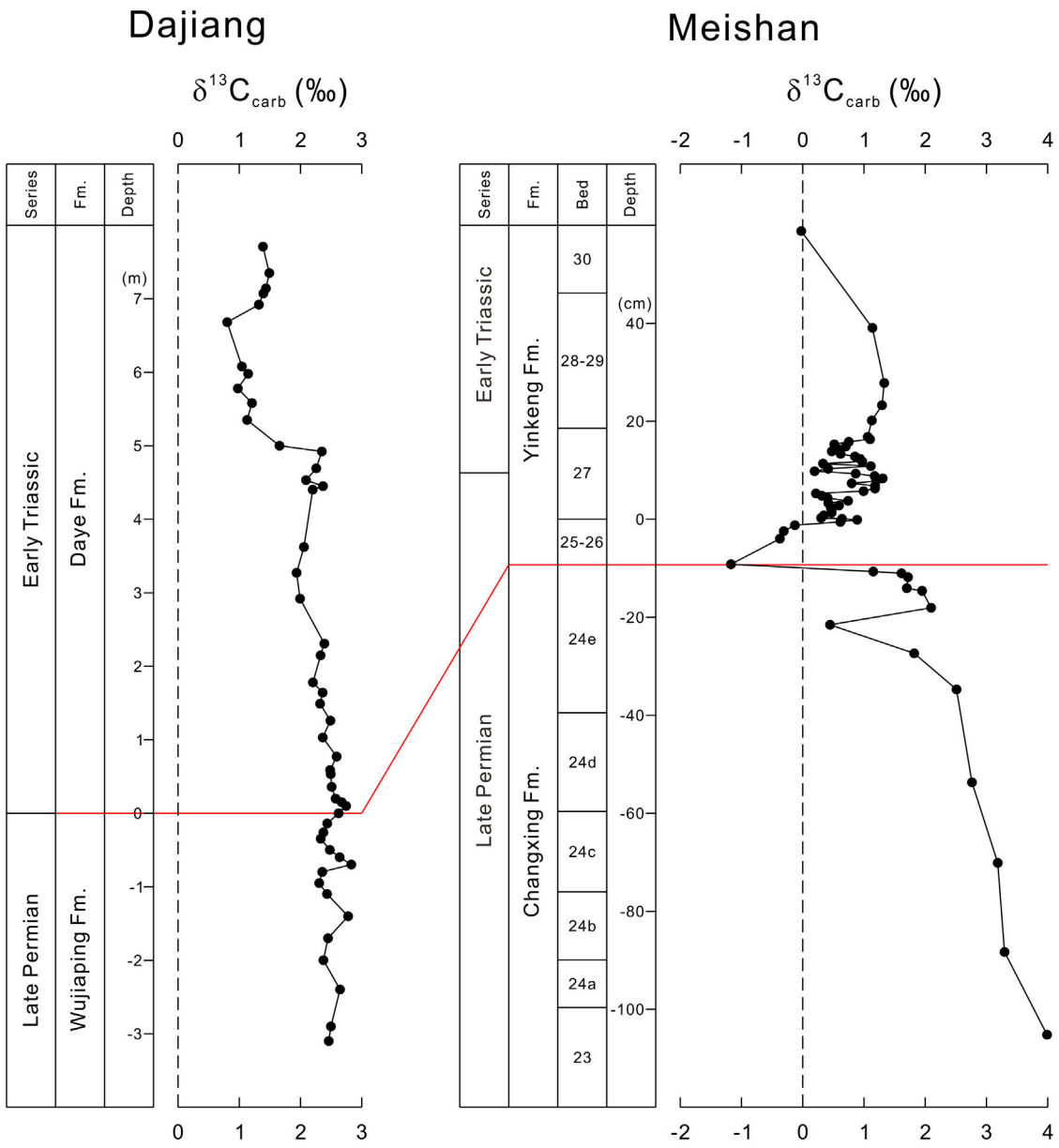

FIGURE 5
Comparison of $\delta^{13}C_{carb}$ records from the Dajiang (this study) and Meishan section (Cao et al., 2002).

extinction skeletal limestones, reflecting complexities of carbon cycling in the basin (Figure 6). The correlations between Dajiang and Cili and Chongyang sections add more complexities of carbon cycling as the late two sections were also deposited in a carbonate platform close to the Northern Deepwater Basin (Luo et al., 2014). Like the Dajiang section, the $\delta^{13}C_{carb}$ profile at Cili shows a general decrease to −0.4‰ and consists of three minor negative $\delta^{13}C_{carb}$ excursions (Figure 6). However, the Chongyang section, which was deposited in a similar environment as the Cili section (Luo et al., 2014), shows relatively stable $\delta^{13}C_{carb}$ values around −0.3‰, after the decrease of about 2‰ from the pre-extinction skeletal limestones (Figure 6).

It appears that there is a general $\delta^{13}C_{carb}$ decrease from the pre-extinction skeletal limestones to the microbialites in all studied sections, although the absolute $\delta^{13}C_{carb}$ decrease varies between each section (Figure 6). After this general $\delta^{13}C_{carb}$ decrease, the $\delta^{13}C_{carb}$ profile of the microbialite either remains relatively stable or continues to decrease (Figure 6). The $\delta^{13}C_{carb}$ value then increases starting from either within the microbialite or after

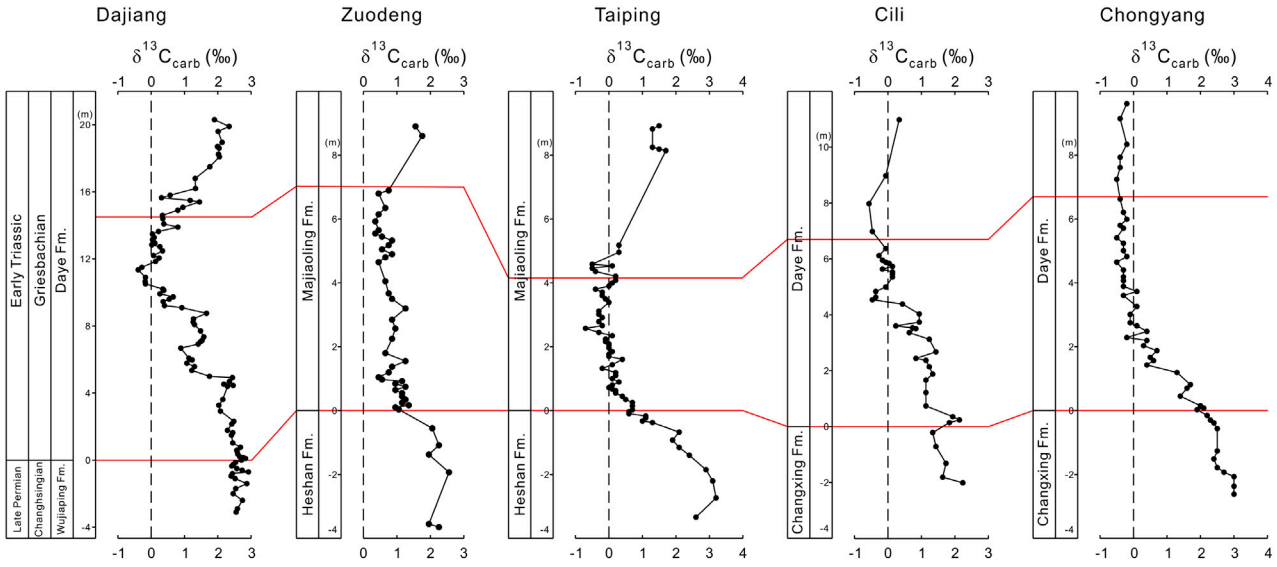

FIGURE 6
Comparison of $\delta^{13}C_{carb}$ records during the Permian-Triassic transition in South China. The data are from the Dajiang (this study), Zuodeng (Luo et al., 2011), Taiping (Luo et al., 2011), Cili (Luo et al., 2011), and Chongyang (Luo et al., 2011) section. The red lines indicate the onset and termination of the microbialite interval.

the microbialite deposition (Figure 6). However, this $\delta^{13}C_{carb}$ increase was not shown in the Chongyang section (Figure 6).

Regardless, the significant $\delta^{13}C_{carb}$ decrease from the pre-extinction skeletal limestones to the microbialites in all studied sections requires inputs of ^{13}C-depleted dissolved carbon. Continental weathering of ^{13}C-depleted carbon was unlikely a major source as a large amount of clastic inputs would have inhibited the growth of microbialite. Likewise, dissociation of methane hydrates was unlikely a major source considering the continuous decreasing $\delta^{13}C_{carb}$ compositions as at Dajiang, as well as the very shallow water environment for precipitation of microbialites. There are possible ^{13}C-depleted sources that could help to explain the decreasing $\delta^{13}C_{carb}$ values for the microbialites. Emission of CO_2 and possibly methane as well by the Siberian Traps magmatism could provide ^{13}C-depleted carbon, producing the negative $\delta^{13}C_{carb}$ excursion (Burgess and Bowring, 2015). Upwelling of anoxic deep water into the photic zone could also contribute ^{13}C-depleted carbon during the microbialite formation (e.g., Kershaw et al., 2007). As well, low productivity could possibly lead to ^{13}C-depleted isotopic values in surface waters. However, evidence for either of the mechanisms may be circumstantial and neither of them can independently explain the negative $\delta^{13}C_{carb}$ excursion from the pre-extinction skeletal limestone to the microbialite level, as well as the differences in $\delta^{13}C_{carb}$ minimums amongst the microbialites deposited in various paleogeographic locations (Figure 6).

The general increasing $\delta^{13}C_{carb}$ profiles within the microbialite interval at Dajiang or after the deposition of the microbialtes elsewhere (Figure 6) suggest changes of carbon cycling in the post-microbialite oceans. Increasing primary productivity and/or anoxia could facilitate enhanced burial of organic carbon, resulting in the increasing $\delta^{13}C_{carb}$ compositions. We speculate that the cessation of microbialites in South China may be linked to the changes of carbon cycling which may have controlled by global and local environmental changes.

Conclusion

The $\delta^{13}C_{carb}$ data from the Dajiang section reveal a general decrease of ~3.2‰ from pre-extinction skeletal limestone to the microbialite deposition. Unlike the $\delta^{13}C_{carb}$ data from many sections in South China, the decreasing $\delta^{13}C_{carb}$ at Dajiang is followed by an increasing $\delta^{13}C_{carb}$ profile. We suggest that multiple sources of ^{13}C-depleted dissolved carbon may be possibly required to explain the decreasing $\delta^{13}C_{carb}$ during the microbialite formation. There is little doubt that carbon cycling during the microbialite precipitation are more complex than previously thought. Though great details about morphology and mineralogical compositions have been studied, local environments for microbialite formation have not been well reconstructed. Future studies should focus on environmental reconstruction for microbialite formation and their possible link to the delayed recovery from the end-Permian mass extinction.

Data availability statement

The original contributions presented in the study are included in the article/Supplementary Material, further inquiries can be directed to the corresponding authors.

Author contributions

YS conceived the study. XZ and YS collected samples. XH, XZ, and ML wrote the manuscript with inputs from DL, YX, LS, and YS.

Funding

This study was supported by the National Natural Science Foundation of China (41721002 and 41890842) and the 111 project (B14026).

Acknowledgments

We dedicated this paper to the late Yongbiao Wang for his pioneering work on the microbialite in South China and his help in collecting samples from Dajiang. We thank Steve Grasby, Haishui Jiang and the reviewers for their constructive comments.

Conflict of interest

The authors declare that the research was conducted in the absence of any commercial or financial relationships that could be construed as a potential conflict of interest.

Publisher's note

All claims expressed in this article are solely those of the authors and do not necessarily represent those of their affiliated organizations, or those of the publisher, the editors and the reviewers. Any product that may be evaluated in this article, or claim that may be made by its manufacturer, is not guaranteed or endorsed by the publisher.

Supplementary material

The Supplementary Material for this article can be found online at: https://www.frontiersin.org/articles/10.3389/feart.2022.914432/full#supplementary-material.

References

Baud, A., Richoz, S., and Pruss, S. (2007). The lower Triassic anachronistic carbonate facies in space and time. *Glob. Planet. Change* 55, 81–89. doi:10.1016/j.gloplacha.2006.06.008

Burgess, S. D., and Bowring, S. A. (2015). High-precision geochronology confirms voluminous magmatism before, during, and after Earth's most severe extinction. *Sci. Adv.* 1, e1500470. doi:10.1126/sciadv.1500470

Burgess, S. D., Muirhead, J. D., and Bowring, S. A. (2017). Initial pulse of Siberian Traps sills as the trigger of the end-Permian mass extinction. *Nat. Commun.* 8, 164. doi:10.1038/s41467-017-00083-9

Cao, C., Love, G. D., Hays, L. E., Wang, W., Shen, S., Summons, R. E., et al. (2009). Biogeochemical evidence for euxinic oceans and ecological disturbance presaging the end-Permian mass extinction event. *Earth Planet. Sci. Lett.* 281, 188–201. doi:10.1016/j.epsl.2009.02.012

Cao, C., Wang, W., and Jin, Y. (2002). Carbon isotope excursions across the permian-triassic boundary in the meishan section, zhejiang Province, China. *Chin. Sci. Bull.* 47, 1125–1129. doi:10.1360/02tb9252

Deng, B., Wang, Y., Woods, A., Li, S., Li, G., Chen, W., et al. (2017). Evidence for rapid precipitation of calcium carbonate in South China at the beginning of Early Triassic. *Palaeogeogr. Palaeoclimatol. Palaeoecol.* 474, 187–197. doi:10.1016/j.palaeo.2016.06.007

Fielding, C. R., Frank, T. D., McLoughlin, S., Vajda, V., Mays, C., Tevyaw, A. P., et al. (2019). Age and pattern of the southern high-latitude continental end-Permian extinction constrained by multiproxy analysis. *Nat. Commun.* 10, 385. doi:10.1038/s41467-018-07934-z

Grasby, S. E., Beauchamp, B., Embry, A., and Sanei, H. (2013). Recurrent early triassic ocean anoxia. *Geology* 41, 175–178. doi:10.1130/G33599.1

Grasby, S. E., and Beauchamp, B. (2008). Intrabasin variability of the carbon-isotope record across the permian-triassic transition, sverdrup basin, arctic Canada. *Chem. Geol.* 253, 141–150. doi:10.1016/j.chemgeo.2008.05.005

Grasby, S. E., Sanei, H., and Beauchamp, B. (2011). Catastrophic dispersion of coal fly ash into oceans during the latest Permian extinction. *Nat. Geosci.* 4, 104–107. doi:10.1038/ngeo1069

Holser, W. T., Schonlaub, H. P., Attrep, M., Boeckelmann, K., Klein, P., Magaritz, M., et al. (1989). A unique geochemical record at the Permian-Triassic boundary. *Nature* 337, 39–44. doi:10.1038/337039a0

Jiang, H., Lai, X., Sun, Y., Wignall, P. B., Liu, J., Yan, C., et al. (2014). Permian-Triassic conodonts from Dajiang (Guizhou, South China) and their implication for the age of microbialite deposition in the aftermath of the end-Permian mass extinction. *J. Earth Sci.* 25, 413–430. doi:10.1007/s12583-014-0444-4

Kamo, S. L., Czamanske, G. K., Amelin, Y., Fedorenko, V. A., Davis, D., Trofimov, V., et al. (2003). Rapid eruption of Siberian flood-volcanic rocks and evidence for coincidence with the Permian-Triassic boundary and mass extinction at 251 Ma. *Earth Planet. Sci. Lett.* 214, 75–91. doi:10.1016/S0012-821X(03)00347-9

Kaufman, A. J., and Knoll, A. H. (1995). Neoproterozoic variations in the C-isotopic composition of seawater: Stratigraphic and biogeochemical implications. *Precambrian Res.* 73, 27–49. doi:10.1016/0301-9268(94)00070-8

Kershaw, S., Crasquin-soleau, S., Li, Y., Collin, P-Y., Forel, M-B., Mu, X., et al. (2012). Microbialites and global environmental change across the permian-triassic boundary: A synthesis. *Geobiology* 10, 25–47. doi:10.1111/j.1472-4669.2011.00302.x

Kershaw, S., Li, Y., Crasquin-soleau, S., Feng, Q., Mu, X., Collin, P-Y., et al. (2007). Earliest triassic microbialites in the South China block and other areas: Controls on their growth and distribution. *Facies* 53, 409–425. doi:10.1007/s10347-007-0105-5

Knoll, A. H., Bambach, R. K., Payne, J. L., Pruss, S., and Fischer, W. W. (2007). Paleophysiology and end-Permian mass extinction. *Earth Planet. Sci. Lett.* 256, 295–313. doi:10.1016/j.epsl.2007.02.018

Krull, E. S., Lehrmann, D. J., Druke, D., Kessel, B., Yu, Y., Li, R., et al. (2004). Stable carbon isotope stratigraphy across the Permian-Triassic boundary in shallow marine carbonate platforms, Nanpanjiang Basin, south China. *Palaeogeogr. Palaeoclimatol. Palaeoecol.* 204, 297–315. doi:10.1016/S0031-0182(03)00732-6

Lehrmann, D. J., Bentz, J. M., Wood, T., Goers, A., Dhillon, R., Akin, S., et al. (2015). Environmental controls on the Genesis of marine microbialites and dissolution surface associated with the end-permian mass extinction: New sections and observations from the Nanpanjiang Basin, south China. *Palaios* 30, 529–552. doi:10.2110/palo.2014.088

Lehrmann, D. J. (1999). Early triassic calcimicrobial mounds and biostromes of the Nanpanjiang Basin, south China. *Geology* 27, 359–362. doi:10.1130/0091-7613(1999)027<0359:etcmab>2.3.co;2

Lehrmann, D. J., Payne, J. L., Felix, S. V., Dillett, P. M., Wang, H., Yu, Y., et al. (2003). Permian-triassic boundary sections from shallow-marine carbonate platforms of the Nanpanjiang Basin, south China: Implications for oceanic conditions associated with the end-permian extinction and its aftermath. *Palaios* 18, 138–152. doi:10.1669/0883-1351(2003)18<138:pbsfsc>2.0.co;2

Li, M., Frank, T. D., Xu, Y., Fielding, C. R., Gong, Y., Shen, Y., et al. (2022). Sulfur isotopes link atmospheric sulfate aerosols from the Siberian Traps outgassing to the end-Permian extinction on land. *Earth Planet. Sci. Lett.* 592, 117634. doi:10.1016/j.epsl.2022.117634

Li, M., Grasby, S. E., Wang, S., Zhang, X., Wasylenki, L. E., Xu, Y., et al. (2021). Nickel isotopes link Siberian Traps aerosol particles to the end-Permian mass extinction. *Nat. Commun.* 12, 2024. doi:10.1038/s41467-021-22066-7

Liao, W., Wang, Y., Kershaw, S., Weng, Z., and Yang, H. (2010). Shallow-marine dysoxia across the permian-triassic boundary: Evidence from pyrite framboids in the microbialite in South China. *Sediment. Geol.* 232, 77–83. doi:10.1016/j.sedgeo.2010.09.019

Liu, H., Wang, Y., Yuan, A., Yang, H., Song, H., Zhang, S., et al. (2010). Ostracod fauna across the Permian-Triassic boundary at Chongyang, Hubei Province, and its implication for the process of the mass extinction. *Sci. China Earth Sci.* 53, 810–817. doi:10.1007/s11430-010-0045-8

Luo, G., Algeo, T. J., Huang, J., Zhou, W., Wang, Y., Yang, H., et al. (2014). Vertical $\delta^{13}C_{org}$ gradients record changes in planktonic microbial community composition during the end-Permian mass extinction. *Palaeogeogr. Palaeoclimatol. Palaeoecol.* 396, 119–131. doi:10.1016/j.palaeo.2014.01.006

Luo, G., Kump, L. R., Wang, Y., Tong, J., Arthur, M. A., Yang, H., et al. (2010). Isotopic evidence for an anomalously low oceanic sulfate concentration following end-Permian mass extinction. *Earth Planet. Sci. Lett.* 300, 101–111. doi:10.1016/j.epsl.2010.09.041

Luo, G., Wang, Y., Yang, H., Algeo, T., Kump, L., and Huang, J. (2011). Stepwise and large-magnitude negative shift in $\delta^{13}C_{carb}$ preceded the main marine mass extinction of the Permian-Triassic crisis interval. *Palaeogeogr. Palaeoclimatol. Palaeoecol.* 299, 70–82. doi:10.1016/j.palaeo.2010.10.035

Meyer, K. M., Yu, M., Jost, A. B., Kelley, B. M., and Payne, J. L. (2011). $\delta^{13}C$ evidence that high primary productivity delayed recovery from end-Permian mass extinction. *Earth Planet. Sci. Lett.* 302, 378–384. doi:10.1016/j.epsl.2010.12.033

Mu, X., Kershaw, S., Li, Y., Guo, L., Qi, Y., Reynolds, A., et al. (2009). High-resolution carbon isotope changes in the Permian-Triassic boundary interval, Chongqing, South China; implications for control and growth of earliest Triassic microbialites. *J. Asian Earth Sci.* 36, 434–441. doi:10.1016/j.jseaes.2007.08.004

Payne, J. L., and Kump, L. R. (2007). Evidence for recurrent Early Triassic massive volcanism from quantitative interpretation of carbon isotope fluctuations. *Earth Planet. Sci. Lett.* 256, 264–277. doi:10.1016/j.epsl.2007.01.034

Payne, J. L., Lehrmann, D. J., Follet, D., Seibel, M., Kump, L. R., Riccardi, A., et al. (2007). Erosional truncation of uppermost Permian shallow-marine carbonates and implications for Permian Triassic boundary events. *Geol. Soc. Am. Bull.* 119, 771–784. doi:10.1130/B26091.1

Payne, J. L., Lehrmann, D. J., Wei, J. Y., Orchard, M. J., Schrag, D. P., Knoll, A. H., et al. (2004). Large perturbations of the carbon cycle during recovery from the end-Permian extinction. *Science* 305, 506–509. doi:10.1126/science.1097023

Pei, Y., Chen, Z., Fang, Y., Kershaw, S., Wu, S., Luo, M., et al. (2019). Volcanism, redox conditions, and microbialite growth linked with the end-Permian mass extinction: Evidence from the Xiajiacao section (Western Hubei Province), South China. *Palaeogeogr. Palaeoclimatol. Palaeoecol.* 519, 194–208. doi:10.1016/j.palaeo.2017.07.020

Riccardi, A., Kump, L. R., Arthur, M. A., and D'Hondt, S. (2007). Carbon isotopic evidence for chemocline upward excursions during the end-Permian event. *Palaeogeogr. Palaeoclimatol. Palaeoecol.* 248, 73–81. doi:10.1016/j.palaeo.2006.11.010

Ryskin, G. (2003). Methane-driven oceanic eruptions and mass extinctions. *Geology* 31, 741–744. doi:10.1130/G19518.1

Shen, J., Schoepfer, S. D., Feng, Q., Zhou, L., Yu, J., Song, H., et al. (2015). Marine productivity changes during the end-Permian crisis and Early Triassic recovery. *Earth. Sci. Rev.* 149, 136–162. doi:10.1016/j.earscirev.2014.11.002

Shen, Y., Farquhar, J., Zhang, H., Masterson, A., Zhang, T., Wing, B. A., et al. (2011). Multiple S-isotopic evidence for episodic shoaling of anoxic water during Late Permian mass extinction. *Nat. Commun.* 2, 210. doi:10.1038/ncomms1217

Song, H., Tong, J., Algeo, T. J., Horacek, M., Qiu, H., Song, H., et al. (2013). Large vertical $\delta^{13}C_{DIC}$ gradients in Early Triassic seas of the South China craton: Implications for oceanographic changes related to Siberian Traps volcanism. *Glob. Planet. Change* 105, 7–20. doi:10.1016/j.gloplacha.2012.10.023

Song, H., Wignall, P. B., and Dunhill, A. M. (2018). Decoupled taxonomic and ecological recoveries from the Permo-Triassic extinction. *Sci. Adv.* 4, eaat5091. doi:10.1126/sciadv.aat5091

Song, H., Wignall, P. B., Tong, J., and Yin, H. (2012). Two pulses of extinction during the Permian-Triassic crisis. *Nat. Geosci.* 6, 52–56. doi:10.1038/ngeo1649

Svensen, H., Planke, S., Polozov, A. G., Schmidbauer, N., Corfu, F., Podladchikov, Y. Y., et al. (2009). Siberian gas venting and the end-Permian environmental crisis. *Earth Planet. Sci. Lett.* 277, 490–500. doi:10.1016/j.epsl.2008.11.015

Wang, L., Wignall, P. B., Wang, Y., Jiang, H., Sun, Y., Li, G., et al. (2016). Depositional conditions and revised age of the permo-triassic microbialites at gaohua section, Cili county (hunan Province, south China). *Palaeogeogr. Palaeoclimatol. Palaeoecol.* 443, 156–166. doi:10.1016/j.palaeo.2015.11.032

Wang, Q., Tong, J., Song, H., and Yang, H. (2009). Ecological evolution across the permian/triassic boundary at the kangjiaping section in Cili county, hunan Province, China. *Sci. China Ser. D-Earth. Sci.* 52, 797–806. doi:10.1007/s11430-009-0077-0

Wang, T., Burne, R. V., Yuan, A., Wang, Y., and Yi, Z. (2019). The evolution of microbialite forms during the early triassic transgression: A case study in Chongyang of hubei Province, south China. *Palaeogeogr. Palaeoclimatol. Palaeoecol.* 519, 209–220. doi:10.1016/j.palaeo.2018.01.043

Wang, Y., Tong, J., Wang, J., and Zhou, X. (2005). Calcimicrobialite after end-Permian mass extinction in South China and its palaeoenvironmental significance. *Chin. Sci. Bull.* 50, 665–671. doi:10.1360/982004-323

Wignall, P. B., Kershaw, S., Collin, P. Y., and Crasquin, S. S. (2009). Erosional truncation of uppermost permian shallow-marine carbonates and implications for permian-triassic boundary events: Comment. *Geol. Soc. Am. Bull.* 121, 954–956. doi:10.1130/B26424.1

Wu, S., Chen, Z., Fang, Y., Pei, Y., Yang, H., Ogg, J., et al. (2017). A Permian-Triassic boundary microbialite deposit from the eastern Yangtze Platform (Jiangxi Province, South China): Geobiologic features, ecosystem composition and redox conditions. *Palaeogeogr. Palaeoclimatol. Palaeoecol.* 486, 58–73. doi:10.1016/j.palaeo.2017.05.015

Xie, S., Pancost, R. D., Huang, J., Wignall, P. B., Yu, J., Tang, X., et al. (2007). Changes in the global carbon cycle occurred as two episodes during the Permian-Triassic crisis. *Geology* 35, 1083–1086. doi:10.1130/G24224A.1

Xie, S., Pancost, R. D., Wang, Y., Yang, H., Wignall, P. B., Luo, G., et al. (2010). Cyanobacterial blooms tied to volcanism during the 5 m.y. Permo-Triassic biotic crisis. *Geology* 38, 447–450. doi:10.1130/g30769.1

Yang, H., Chen, Z., Wang, Y., Tong, J., Song, H., Chen, J., et al. (2011). Composition and structure of microbialite ecosystems following the end-Permian mass extinction in South China. *Palaeogeogr. Palaeoclimatol. Palaeoecol.* 308, 111–128. doi:10.1016/j.palaeo.2010.05.029

Yin, H., Jiang, H., Xia, W., Feng, Q., Zhang, N., Shen, J., et al. (2014). The end-Permian regression in South China and its implication on mass extinction. *Earth. Sci. Rev.* 137, 19–33. doi:10.1016/j.earscirev.2013.06.003

Yin, H., Zhang, K., Tong, J., Yang, Z., and Wu, S. (2001). The global stratotype section and point (GSSP) of the Permian-Triassic boundary. *Episodes* 24, 102–114. doi:10.18814/epiiugs/2001/v24i2/004

Zhang, G., Zhang, X., Hu, D., Li, D., Algeo, T. J., Farquhar, J., et al. (2017). Redox chemistry changes in the Panthalassic Ocean linked to the end-Permian mass extinction and delayed Early Triassic biotic recovery. *Proc. Natl. Acad. Sci. U. S. A.* 114, 1806–1810. doi:10.1073/pnas.1610931114

Zhang, G., Zhang, X., and Shen, Y. (2021). Quantitative constraints on carbon cycling and temporal changes in episodic euxinia during the end-Permian mass extinction in South China. *Chem. Geol.* 562, 120036. doi:10.1016/j.chemgeo.2020.120036

Zhang, X., Zheng, Q., Li, Y., Yang, H., Zhang, H., Wang, W., et al. (2020). Polybessurus-like fossils as key contributors to Permian-Triassic boundary microbialites in South China. *Palaeogeogr. Palaeoclimatol. Palaeoecol.* 552, 109770. doi:10.1016/j.palaeo.2020.109770